https://doi.org/10.48048/tis.2023.6411

Implications of the Electrodeposition Scan Rate on the Morphology of Polyaniline Layer and the Impedance of a QCM Sensor

Nugrahani Primary Putri[1,2], Evi Suaebah[1], Lydia Rohmawati[1], Dionysius Joseph Djoko Herry Santjojo[2], Masruroh[2,*] and Setyawan Purnomo Sakti[2]

[1]Department of Physics, Faculty of Mathematics and Natural Science, Universitas Negeri Surabaya, Surabaya, Indonesia
[2]Department of Physics, Faculty of Mathematics and Natural Science, Brawijaya University, Malang, Indonesia

([*]Corresponding author's e-mail: ruroh@ub.ac.id)

Received: 28 November 2022, Revised: 3 January 2023, Accepted: 4 January 2023, Published: 6 January 2023

Abstract

This work aims to determine how the scan rate affects PANI layers' morphology and resonance parameters deposited on quartz crystal microbalance (QCM). The PANI layer was produced using the electrodeposition method with a scan rate variation of 10 to 50 mV/s. The PANI layer deposited at a scan rate of 10 mV/s has an aggregate morphology, whereas the morphology becomes more scattered at a higher scan rate. On the other hand, the homogeneity of the distribution of PANI particles increases due to the increase in the scan rate. The QCM impedance profile also changes with PANI layer deposition at different scan rates. The QCM impedance profile with the PANI layer that is most similar to the uncoated QCM impedance profile is at a scan rate of 10, 40 and 50 mV/s. The resonance parameters, which represent the inertial mass and the dissipative characteristics of the PANI layer, were investigated. The PANI layer with the smallest resonance parameter has a scan rate of 10 and 40 mV/s. Therefore, the 2 scan rates are the best candidates to be applied further.

Keywords: Electrodeposition, Polyaniline, QCM, Resonance parameter, Structural

Introduction

The sensor has an important part of modern life. Many sensors require high performance, including increased sensitivity, fast response speed, etc. Quartz crystal microbalance (QCM) is a sensor device with advantages, including high sensitivity and selectivity, fast response, and simple instrumentation. QCM is a device made of a quartz crystal plate with gold (Au) or silver (Ag) electrodes on both sides. When QCM interacts with an analyte, there will be a change in the QCM's resonant frequency due to the addition of mass on its surface. Layer modification by adding active ingredients to the QCM surface was conducted to improve the sensitivity and selectivity of QCM. Several active layer QCM-based sensor devices include TiO_2/Ag composites as humidity sensors [1,2], phthalocyanine as benzene, toluene, and xylene (BTX) sensors [3], PANI/NiO as gelatine detectors [4], and graphene as gas sensors [5]. Due to the characteristics of quartz crystals, microbalance has received increasing attention in this field. Their low cost and digital signal output have special attention and the high value of QCM.

Polyaniline is a conductive polymer that has also been widely applied as a QCM-based sensor [6-10]. The selection of polyaniline (PANI) as a candidate for active sensor material is because PANI has good reversibility, high stability, and is easy to synthesize. PANI deposition methods above QCM are quite diverse, including spin coating [11], drop coating [12], layer-by-layer (LbL) methods [13], evaporation [14], spray methods [15], and electrochemical deposition [16]. Our previous study [16] succeeded in depositing the PANI layer above QCM by varying the deposition scan rate, and obtained the result that the scan rate has an effect on the impedance value. However, this study has not analyzed the relationship between scan rate deposition changes with the morphology of the PANI layer and its resonance properties. The current research is a continuation of the previous research. Nowadays, the electrochemical deposition (electrodeposition) method has been the most promising method for depositing PANI on the QCM surface. The electrodeposition method has many advantages; simple preparation, ease of use, accurate initiation control, and short deposition time. *Electrodeposition* is an electrochemical process that deposits aniline molecules onto QCM substrate through oxidation and reduction processes. Several parameters affect the quality of the thin film resulting from the electrodeposition method, including deposition time, scan rate,

monomer concentration, temperature, pH, current density [17], physical and chemical nature of substrate surface, dopant type [18] and template used in the electrodeposition process [19].

According to the electrodeposition method, the scan rate is one of the leading acting parameters of the film's growth process and hence one of the induced film microstructures, including surface morphology and thickness [20]. Although there are sufficient reports on the electrodeposition techniques for synthesizing the PANI layer on the QCM surface, there are few reports on the effect of scan rate on the structural and resonance properties of the resulting PANI layer produced using electrodeposition. For instance, Baba *et al.* [21] successfully prepared PANI thin film via electrodeposition at QCM substrate to investigate polyaniline thin film's properties. They found that the change in the electrochemical properties of PANI upon the redox process produces a change in surface plasmon resonance response. Mohamoud *et al.* [22] have investigated the mechanical resonance phenomenon during the electrochemical deposition of PANI using electrochemical quartz crystal microbalance (EQCM). This study found that the values of the resonance parameters L2 (representing the effectively coupled inertial mass) and R2 (representing the dissipation of acoustic energy) changed as a function of the electrodeposition cycle. The value of R2 decreases drastically due to the containment of the acoustic energy within the resonating film rather than its partial transmission to an ultimate dissipation within the fluid. However, this study could not explain the decrease in the value of the L2 parameter when the deposition process was in progress.

Compared to other studies that used surface plasmon resonance and EQCM to determine the resonance characteristics of the PANI layer. Here we report that the resonance parameters of the PANI layer at the QCM surface can be determined using a BVD model approach using the non-linear Generalized Reduced Gradient (GRG) method. The novelty of this study is that no research has explained the relationship between scan rate, resonance parameters, and morphology of PANI films. This relationship has an impact on the characteristics of PANI films. This work shows that scan rate variations in the electrodeposition of PANI change the film resonance parameter and surface morphology. We also indicate the correlation between the resonance parameter's value and the homogeneity of PANI film morphology. This observation can further used to guide the optimal process of producing the PANI layer over QCM using the electrodeposition method.

Materials and methods

Materials

Polyaniline film deposition onto QCM surface using electrochemical process performed with a potentiostat-galvanostat Gamry Reference 3000. Aniline ($C_6H_5NH_2$) (analytical grade, Merck) was doped on QCM without pretreatment. Hydrochloric acid (37 %, Merck) was used as an electrolyte in the electrochemical process. All electrochemical processes were performed with the electrode Metrohm Ag/AgCl as a reference electrode. The counter electrode was a platinum wire 0.4 mm in diameter, and the working electrode was Quartz Crystal Microbalance (QCM). This work used a commercially QCM 10 MHz AT-Cut with electrochemically active area A = 0.5 cm^2 silver (Ag) electrodes from Greatmicro Electronic. The front electrode of the crystal was used as the working electrode and the back electrode was grounded.

Polyaniline electrodeposition

Polyaniline films were deposited potentiodynamically (−0.4 - +1.0 V) from an aqueous 0.3 M aniline and 0.5 M HCl solution. Each film deposition was prepared freshly from aniline solution. Each electrodeposition process is carried out with a different scan rate; 10, 20, 30, 40 and 50 mV/s. On one QCM leg, the deposition process was carried out. This leg was placed into the aniline solution and only used for deposition while linked to the Gamry Instrument. PANI will be deposited on the surface of the Ag electrode (front electrode) of the QCM. The next step as a final process of deposition QCM is washed with acetone and dried at 50 °C for 20 min. Schematically the PANI layer electrodeposition process can be seen in **Figure 1**.

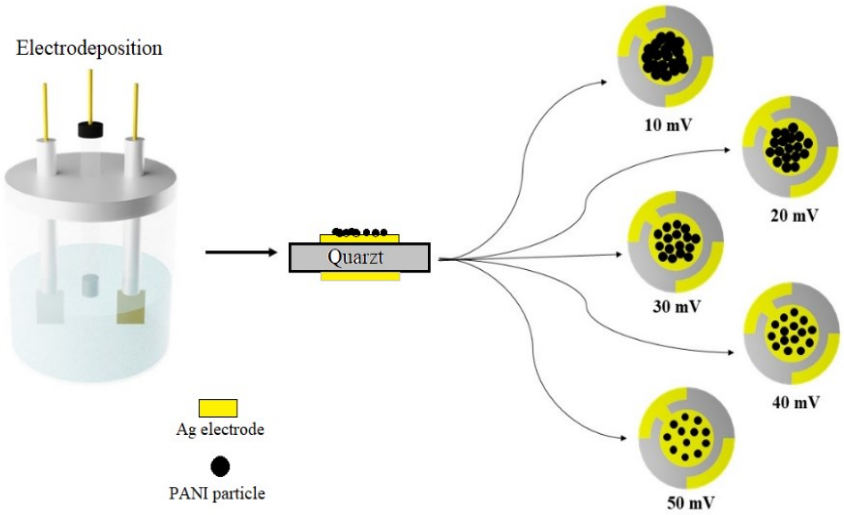

Figure 1 Schematic of the PANI layer electrodeposition process on QCM.

Electrochemical, morphology, and impedance characterization

Electrochemical cell reaction on the QCM surface was conducted by a qualitative and quantitative analytical technique using Cyclic voltammetry. In cyclic voltammetry, the current response is measured as a function of voltage potential, where the potential is applied back and forward. The reduction and oxidation information can be observed properly as back and forward voltage potential. The cyclic voltammetry characteristics depend on the electron transfer reaction rate, electroactive reactivity, and scan rate. I-V curves were obtained during the electrodeposition process, which can provide PANI polymerization information on the QCM surface. The morphology of the PANI film was analyzed using Scanning Electron Microscope (SEM). The energy Dispersion X-ray (EDX) spectrometer was used to analyze the composition of the PANI layer deposition on the QCM surface.

The impedance value of QCM was measured using Omicron Bode 100 Impedance Analyzer to see the viscoelastic and resonance behavior of PANI film before and after PANI coating. The resonance frequency value of the sensor was taken at minimum impedance. Data acquisition was accomplished via a PC running and analyzed using Microsoft excel macro non-linear program with a non-linear Generalized Reduced Gradient (GRG) method to determine the parameter resonance's value.

Result and discussion

Electrochemical properties

The electrochemical behavior of PANI film was investigated by cyclic voltammetry (**Figure 2**). The voltammograms were recorded for one cycle at scan rates 10, 20, 30, 40 and 50 mV/s with a potential range from −0,4V to +1,0V vs. Ag/AgCl. **Figure 2** shows the cyclic voltammograms of the growth of PANI on the QCM electrode from an HCl aqueous acidic solution containing 0.3 M anilines. From the CV characterization, it can be seen that the difference in scan rate affects the CV curve. At a scan rate of 10 mV/s (black curve), there are three oxidation peaks (**Figure 2** peak 1 to 3) at a potential +0.06, +0.34 and +0.68 V, which are peaks due to a phase change from leucoemeraldine (LB) to the emeraldine salt (ES) phase due to insertion of anion, and a phase change from ES to pernigraniline (PB) due to expulsion of protons [23]. The difference in scan rate causes peak positions slightly shift to higher potentials in anodic peaks. At a scan rate of 10 mV/s, the second oxidation peak has a much smaller current than the other scan rates. This indicates a simultaneous phase change from LB to ES (first oxidation peak) and a phase change from ES to PB (third oxidation peak). At a higher scan rate, a second oxidation peak indicates that the phase change from LB to ES does not occur directly but passes through the change from LB to EB (emeraldine base); only then does the phase change from EB to ES occur.

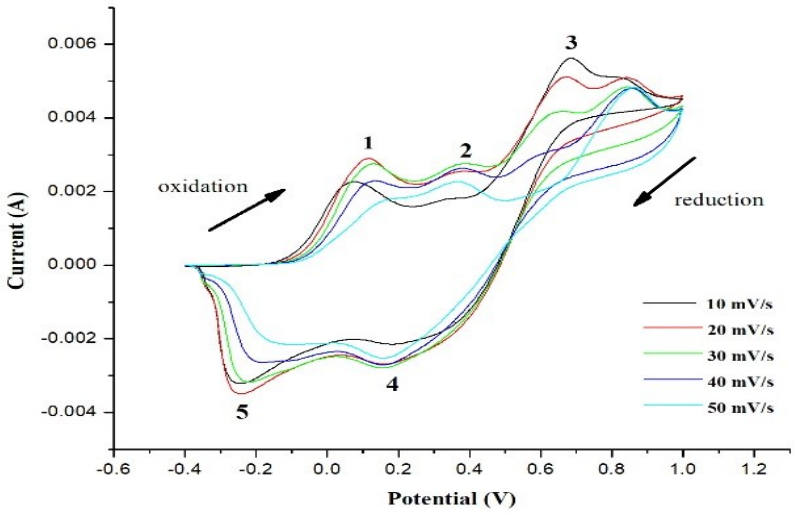

Figure 2 Cyclic voltammograms of QCM electrode in 0.3 M aniline + 0.5 M HCl solution scanned for 1 cycle from −0.4 to +1.0 V at different scan rate.

Two reduction peaks (**Figure 2** peak 4 and 5), indicate the phase change from PB to ES due to the expulsion of anions was observed at +0.2 and −0.22 V. When the scan rate increases, the oxidation and reduction peaks will move toward a positive potential. The voltammogram curve shows that PANI has stable oxidation and reduction reactions. Osmotic equilibrium occurs when there is an ion exchange equilibrium in solution, either in the form of dissolved ions or as free solvent molecules. During the electrochemical reaction, there is a continuous reaction: the insertion of electrons and the extraction of ions from the polymer chain. This behavior indicates quasi-reversible reactions are involved in synthesized PANI [24].

Morphology properties

The surface morphology of the Ag electrode (on the QCM surface) before being coated with PANI can be seen in **Figure 3**. Ag particles have a spherical shape that is neatly arranged with a uniform size. The morphology of PANI layer deposited on the Ag electrode was also observed using SEM and analyzed Image J software for particle size distribution. PANI particles (little bright color) can be seen sticking to the surface of the Ag electrode with uneven distribution, according to the scan rate used in the electrodeposition process. There are differences in the morphology of Ag before deposition and after deposition. After PANI deposition, Ag particles appear larger and form plates (grey color) due to the interaction between Ag and HCl (the dopant used during deposition).

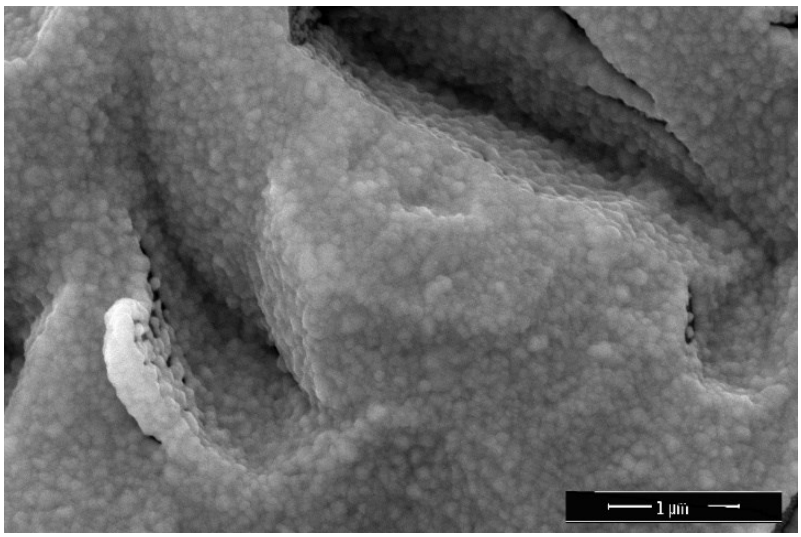

Figure 3 Morphology of QCM uncoated with 20k magnification.

The morphology of the PANI layer deposited on the Ag electrode can be seen in **Figures 4(a) - 4(e)** with 20k magnification, a larger magnification (40k) can be seen in **Figures 4(a) - 4(e)**. **Figures 4(a) - 4(e)** shows that different scan rates have influenced the distribution of PANI particles deposited on the Ag electrode. At low scan rate (**Figure 4(a)**), PANI particles appear to stack on top of each other to form aggregates. The accumulation of PANI particles can be explained because a low scan rate causes a longer deposition time. PANI particles that have already been deposited will be stacked with other PANI particles. With a higher scan rate (less deposition time), PANI particles will be less deposited and more scattered on the Ag electrode (**Figures 4(b) - 4(e)**). When viewed from the particle size distribution by ImageJ (**Figures 4(f) - 4(j)**), the particle size ranges of PANI from 36 to 39 nm. A scan rate of 50 mV/s has the smallest particle size, while a scan rate of 10 mV/s is the largest.

When the oxidation and reduction processes continued simultaneously, some aggregates were found to form during the induction period. The aggregates come immediately before polymerization due to aniline cations and dopant acid anions aggregating. This aggregate then leads to the growth of PANI particles on the Ag electrode. During the nucleation process, the monomers undergo rearrangements that minimize random growth on the Ag electrode surface [25]. The development of the PANI particle on the Ag electrode surface occurs more rapidly and is directly correlated with the scanning rate during the electrodeposition process.

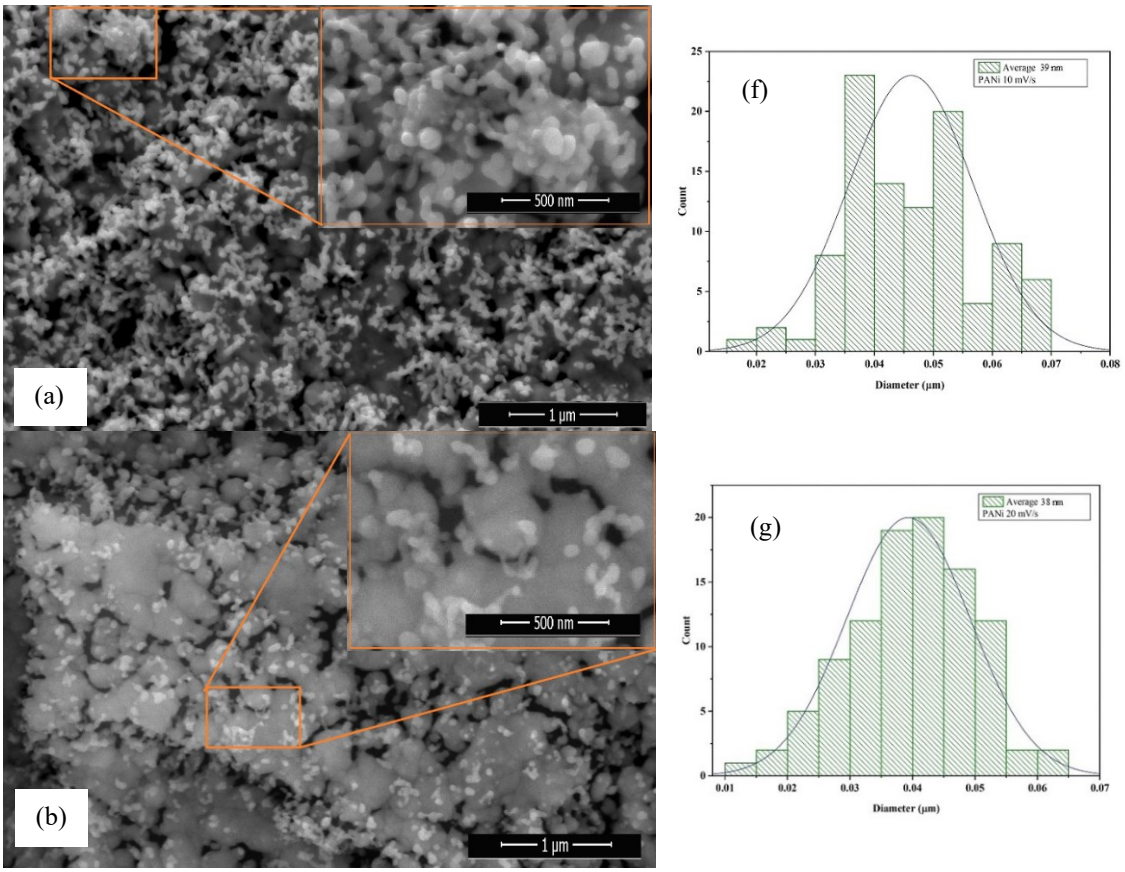

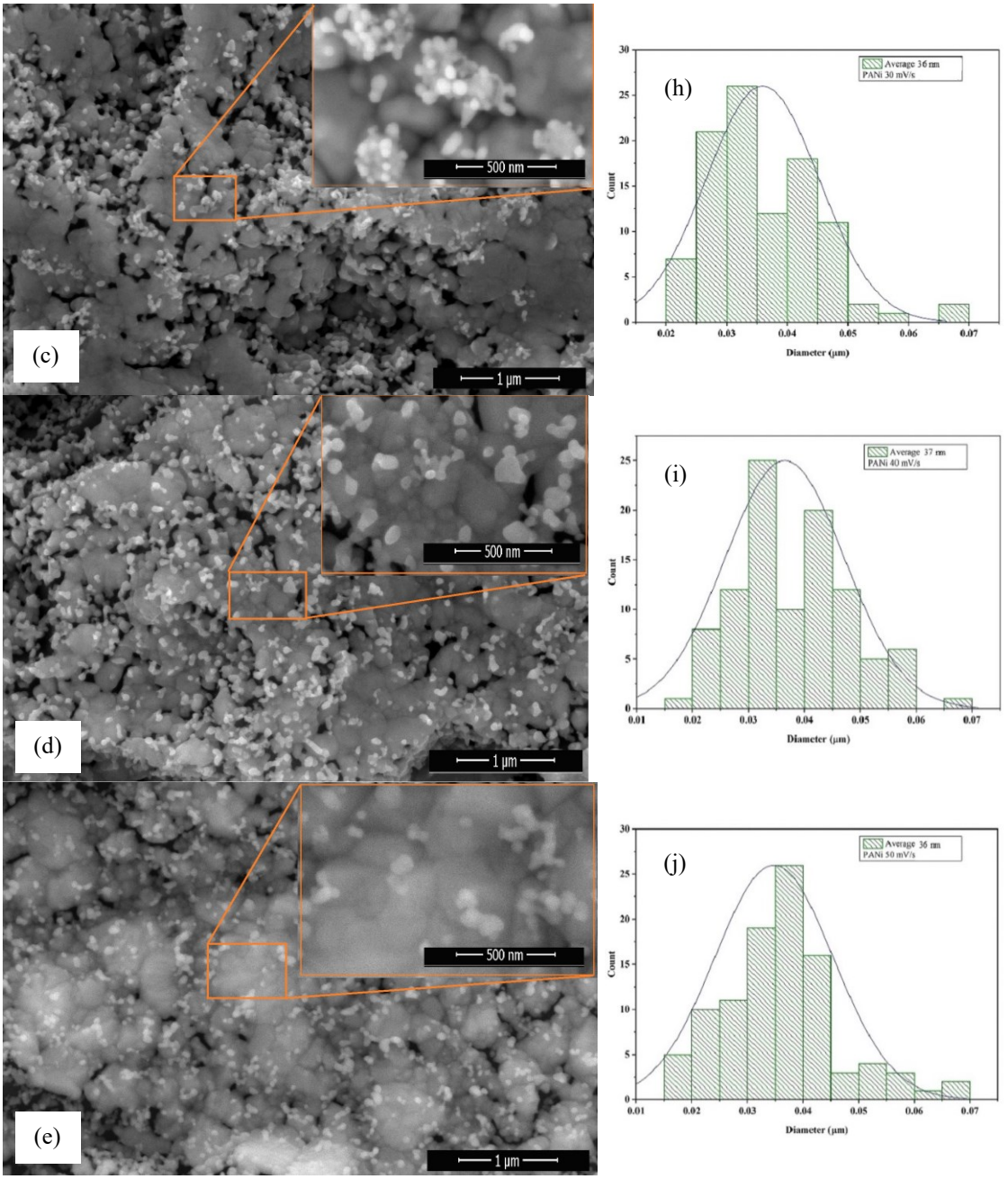

Figure 4 Morphology of PANI layer with different scan rates (a) 10 mV/s, (b) 20 mV/s, (c) 30 mV/s, (d) 40 mV/s and (e) 50 mV/s; and particle size distribution of PANI with different scan rates (f) 10 mV/s, (g) 20 mV/s, (h) 30 mV/s, (i) 40 mV/s and (j) 50 mV/s.

The PANI layer composition test on QCM was carried out using Energy Dispersion X-ray (EDX). **Figures 5(a) - 5(e)** shows the EDX test results for samples with different scan rates. The inset shows particle C distribution. Several elements are detected on the QCM surface, including Si and Ag as the main ingredients of the QCM sensor. Element O was detected as part of quartz (SiO_2) and polyaniline, while elements C and Cl are constituents of polyaniline. With the difference in the scan rate in the electrodeposition method, there are some differences in the content of C and Cl elements, as shown in **Table 1**.

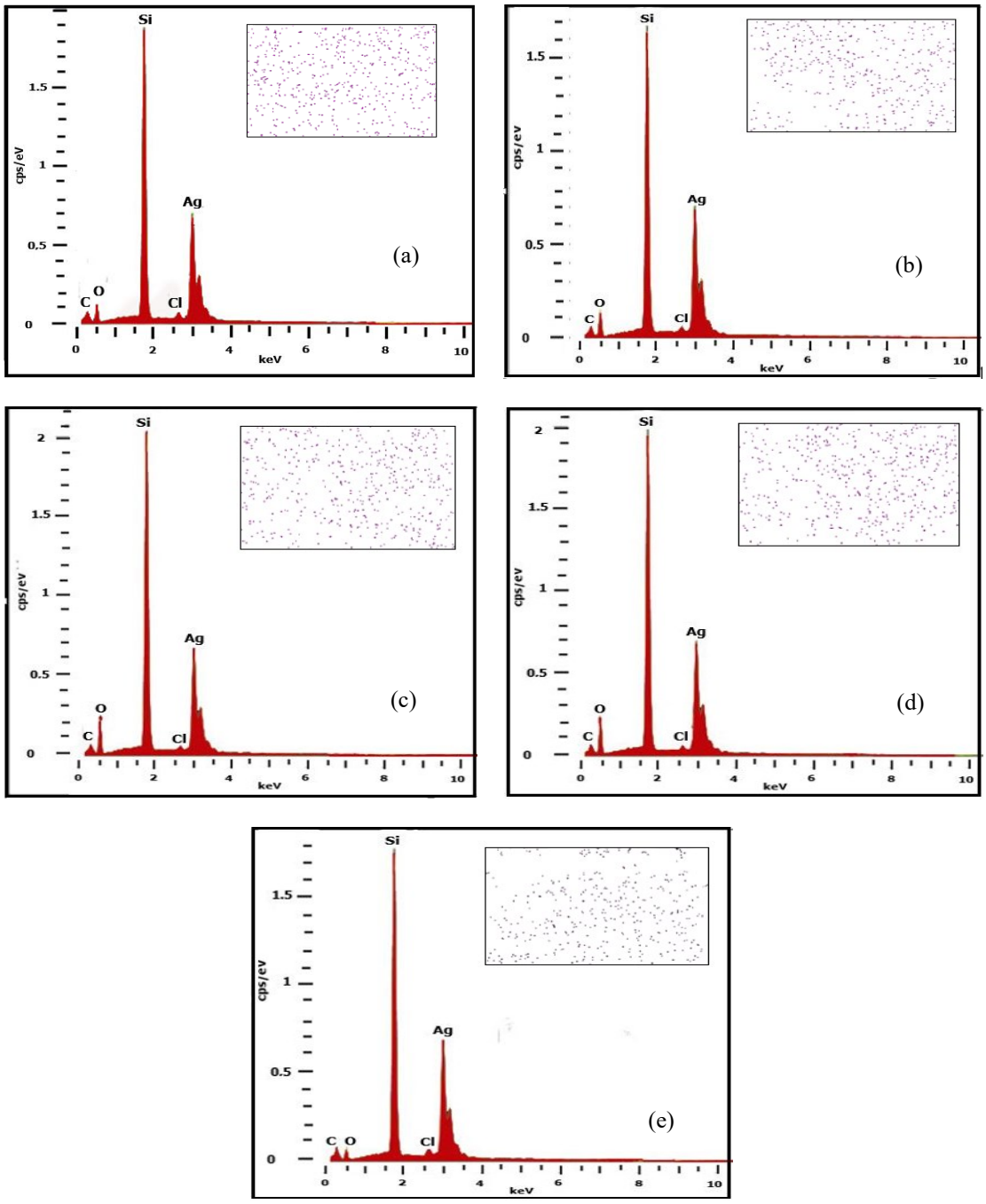

Figure 5 EDX result of PANI layer with different scan rates (a) 10 mV/s; (b) 20 mV/s; (c) 30 mV/s; (d) 40 mV/s and (e) 50 mV/s.

Table 1 shows that different scan rates impact the composition of C and Cl elements on the QCM surface. As discussed above, polyaniline with an emeraldine salt (ES) phase is the result of the protonation of an emeraldine base (EB) with a strong acid. The Cl element appears in the PANI layer deposited above the QCM, which is come from HCL. The concentration of element C in the PANI layer increased according to the scan rate, with the maximum value at 50 mV/s. The presence of the element Cl in the sample varied depending on the scan rate. Due to the low concentration of Cl, the Cl level could not be identified at a scan rate of 20 mV/s. However, the Cl element was significantly detected at a scan rate of 50 mV/s. The results of the composition test using EDX have also proven that the electrodeposition scan rate affects the composition of the PANI layer. The percentage of C element comes highest (22.61 %) at 50 mV/s and lowest (10.05 %) at 10 mV/s.

Table 1 The results of the PANI layer composition test (atomic %).

Element	Scan rate				
	10 mV/s	**20 mV/s**	**30 mV/s**	**40 mV/s**	**50 mV/s**
C	10.05	10.32	10.12	10.51	22.61
Cl	0.48	0	0.05	0.12	0.63

Resonance properties

As a piezoelectric device, the quartz will oscillate at a specific frequency if a potential change is applied to the QCM. Several mathematical models have been proposed to improve the understanding of the resonance properties of QCM. The Butterworth van Dyke (BVD) model is one of the simplest [26]. Based on the physical properties of QCM, the BVD model uses four parameters (**Figure 6 (a)**). The electrical capacitance across the electrodes is C_0, motional inductance is L_Q, emotional resistance is R_Q, and motional capacitance is C_Q [27]. Suppose the surface of the QCM is given a layer of active material, this BVD model must be modified by adding two more parameters, R_P (resistor of PANI layer) and L_P (inductance of PANI layer). Each parameter can describe the damping parameters of QCM due to adding films (**Figure 6 (b)**.

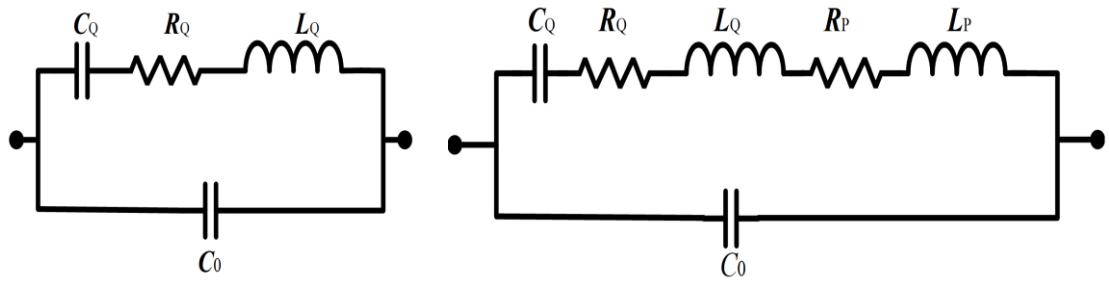

Figure 6 Equivalent circuit based on BVD model of (a) QCM uncoated, and (b) QCM with PANI layer.

Figure 7(a) is a graph of impedance measurements for QCM before coated by PANI. The impedance magnitude graph and the impedance phase are on the same frequency (green circle) indicate the impedance curve without layer. **Figures 7(b) - 7(f)** shows the QCM impedance graph coated with PANI layer with scan rate variations. Each impedance graph consists of the magnitude curve (black line) and the phase curve (red line). It can be seen from **Figure 7** that there is a change in the magnitude and phase curve due to scan rate variations. Significant changes in the impedance curve can be observed on the PANI films deposited with a scan rate of 20 mV/s (**Figure 7(c)**). There is a rounded peak at both magnitude and phase curves. A rounded peak indicates a viscoelastic or elastic character, and the film dissipates some oscillation energy [28]. PANI film deposited at a scan rate of 30 mV/s also has a slightly curved phase peak and a peak magnitude that is not as sharp as other scan rates.

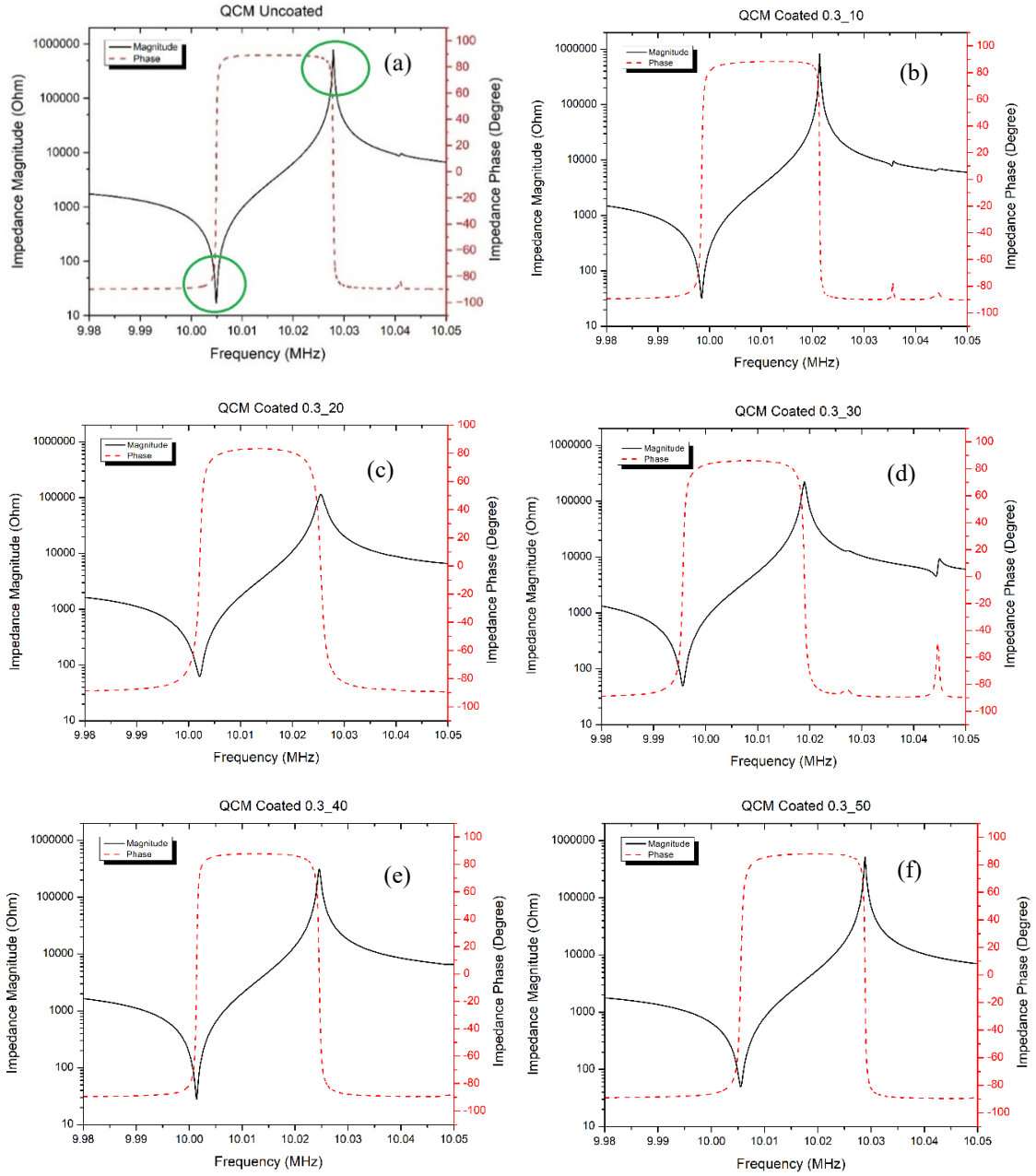

Figure 7 Impedance profile for (a) QCM uncoated; and QCM with PANI layer at the different scan rate (b) 10 mV/s, (c) 20 mV/s, (d) 30 mV/s, (e) 40 mV/s and (f) 50 mV/s.

The impedance profile of QCM with PANI layer at a scan rate of 10 mV/s (**Figure 7(b)**) is similar to the uncoated QCM profile, which indicates that the deposited PANI layer has the properties of a rigid film [29]. In the QCM impedance profile with PANI layer at a scan rate of 30 mV/s (**Figure 7(d)**), the impedance magnitude graph is lower than the impedance phase graph, and the peak impedance magnitude is not as sharp as the peak impedance magnitude graph of uncoated QCM. This difference indicates that the PANI layer deposited at a scan rate of 30 mV/s is less rigid. At a scan rate of 40 mV/s and 50 mV/s (**Figures 7(e)** and **7(f)**), the impedance profile of QCM with PANI layer also has similarities to the impedance profile of uncoated QCM, so it can be said that at a scan rate of 40 and 50 mV/s, the deposited PANI layer has rigid properties.

PANI layer's resonance parameters with scan rate variations can be seen in **Figure 8(a)**. The parameter R_P represents the dissipative properties of the PANI layer. While the parameter L_P represents the inertial mass of the layer, if the value is too large, it will have a loading effect on the QCM. Differences in the R_P and L_P parameters occur from variations in the scan rate. However, the variations in the parameters

do not correspond to the variations in the scan rate. The smallest R_P value was found in PANI film deposited at a scan rate of 40 mV/s, which was 9.93 Ω, while the most considerable R_P value was found in PANI film deposited at a scan rate of 20 mV/s, which was 42.85 Ω. As previously discussed, the PANI film deposited at a scan rate of 20 mV/s has rounded peaks indicating that the film dissipates the oscillation energy. The total resistor value (Rs) obtained from a linear combination between R_Q and R_P is greater than the total L value. A significant increase in the total resistance of the movement arm, compared to the minimal change in inductance, represents the ratio of stored energy to energy lost in each oscillating period of the QCM sensor. This behavior is mainly influenced by the parallel combination of $Rs||C0$, which is close to resonance and no longer dominated by the series combination and greatly affects the maximum or minimum impedance values and phases [30].

If R_P contributes to the shape of the magnitude and phase curve, then the value of L_P will correlate with the mass of PANI deposited in QCM. The largest L_P value is owned by PANI film deposited with a scan rate of 30 mV/s, while the smallest L_P is owned by PANI film with a scan rate of 50 mV/s. The addition of mass on the QCM surface will shift the QCM resonance frequency due to electromechanical mechanisms. The effect of adding mass on the QCM surface follows the following Saurbrey equation:

$$\Delta m = \frac{A\sqrt{\rho_q \mu_q}}{2f_0^2}.\Delta f \quad (1)$$

with Δf is frequency changes (Hz), f_0 is the fundamental resonant frequency of QCM, A is the area of the deposited quartz (m^2), ρ_q is quartz density (2,684 g/cm^3) and μ_q is quartz modulus (2,947×10^{11} g/cm s^2) [31].

The amount of PANI mass deposited can be determined using the Saurbrey equation. **Figure 8(b)** shows that the PANI film's most significant mass is deposited at a scan rate of 30mV/s. This result is consistent with its phase and impedance curve (**Figure 7(d)**). The smallest mass deposition was obtained in samples with a scan rate of 50 mV/s. The sample curve at a scan rate of 50 mV/s can be seen in **Figure 7(f)**. The phase curve and the magnitude curve of PANI film are similar to the QCM uncoated phase and magnitude curves (**Figure 7(a)**), with nearly the same resonant frequency and similar curve shapes.

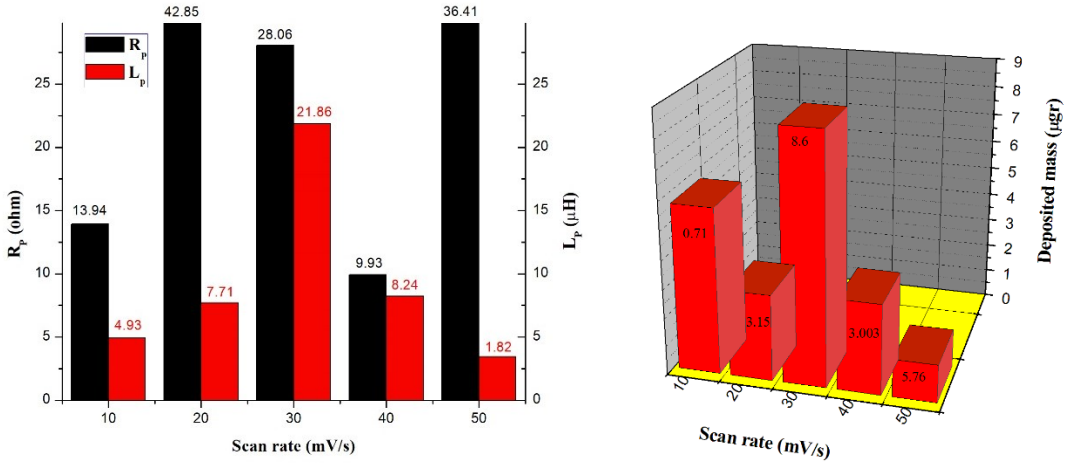

Figure 8 Scan rate effect on (a) PANI layer's resonance parameters and (b) PANI deposited mass at QCM.

Discussion

The cyclic voltammetry result shows that the scan rate effect the electrochemical properties of PANI layer. The current density of the oxidation peak decreases with the scan rate, as shown in **Figure 9**, which relates to the growth of the electroactive PANI layer on the QCM substrate. The decrease in current density can be explained by its proportionality to the concentration of the aniline monomer [32]. The decrease in current density as the scan rate increases will cause differences in the morphology of the PANI films deposited on the QCM. The scanning electron microscope image shows that with a higher scan rate, fewer PANI particles will be deposited on the QCM. The mechanism of PANI film formation on the QCM surface can be explained as follows. Starting from the non-oxidized PANI chain (LB form) attached to the surface of the Ag electrode, 2 electrons move to the electrode and release two ions (H+). The positive charge can

move along the monomer chain and return to its initial reduced state. Increasing the scan rate can speed up the process and lead to forming a PB phase that can no longer transfer charge [33]. The processes are also complicated by the anions which intercalate into PANI film due to diffusion and migration caused by the electric field.

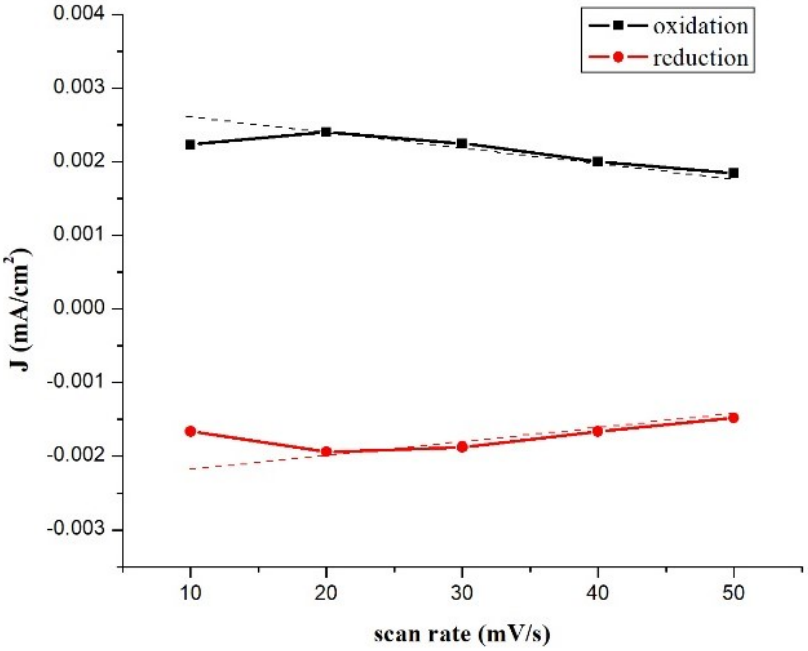

Figure 9 Scan rate effect on current density.

There is a correlation between the morphology of the PANI layer and the determination of the value of the resonance parameter R_P. From the morphology results for a scan rate of 10 mV/s (**Figure 4(a)**) and a scan rate of 40 mV/s (**Figure 4(d)**), it can be seen that there is a similarity in the distribution of PANI particles. PANI particles have a more aggregate morphology than the other three scan rates. The differences are consistent with the determination of the value of R_P (**Figure 8(a)**), where the scan rate of 10 and 40 mV/s has a smaller R_P value than other scan rates. From this, it can be concluded that the morphology of the deposited PANI particles influences the value of R_P. Aggregated PANI particles will have a smaller R_P value than scattered PANI particles.

There is a correlation between the L_P value and the distribution of PANI particles on the Ag electrode surface when we look at the results of determining the resonance parameters and the results of morphological observations. At a scan rate of 30 mV/s, the morphology of the PANI particles was seen to be stacked, which correlated with a significant L_P value. In contrast side, a minimal L_P value can adequately explain relatively few PANI particles deposited at a scan rate of 50 mV/s. The distribution of PANI particles at a scan rate of 10 mV/s is also stacked up to form an agglomerate. Still, the accumulation occurred on almost the entire Ag electrode surface, which caused the PANI mass to be evenly distributed.

Conclusions

According to the research, the electrochemical characteristics, morphology, and resonance characteristics of the PANI layer are all directly influenced by the variation in scan rate during the electrodeposition process of the PANI film above QCM. This work successfully explains the link between scan rate, PANI layer morphology, and PANI layer resonance parameters. The significant scan rate will affect the structure and resonance parameters of the PANI film. At a high scan rate, the deposited PANI particles will be less than at a low scan rate, which will affect the value of the resonance parameter. Scan rates of 10 and 40 mV/s have the best performance because they have an aggregate PANI morphology and small resonance parameters so they can be recommended for applications such as sensors.

Acknowledgements

The authors would like to thanks LPPM Universitas Negeri Surabaya, Indonesia for their financial contribution to this research and the Central Laboratory of Life Sciences (LSIH) Brawijaya University, Indonesia for providing excellent service to support this research. A part of this research also supported by Hibah doktor lektor kepala grant, FMIPA, Brawijaya University, Indonesia.

References

[1] X Zhao, X Chen, F Liu, X Ding, X Yu, K Tang and G Li. An ultrafast QCM humidity sensor for respiratory monitoring outside a mask. *Sensors Actuators B Chem.* 2022; **371**, 132396.

[2] A Biadasz, M Kotkowiak, D Łukawski, J Jadwizak, K Rytel and Kędzierski. A versatile gas transmission device with precise humidity control for QCM humidity sensor characterizations. *Measurement* 2022; **200**, 111674.

[3] A Kumar, C Varenne, A L Ndiaye, A Pauly, M Bouvet and J Brunet. Improvement in metrological performances of phthalocyanine-based QCM sensors for BTX detection in air through substituent's effect. *Sensors Actuators B Chem.* 2022; **368**, 132253.

[4] F Kurniawan, A Nugroho, R A Baskara, L Candle, D Pradini, KA Madurani, RD Sugiarso and H Juwono. Rapid analysis to distinguish porcine and bovine gelatin using PANI/NiO nanoparticles modified Quartz Crystal Microbalance (QCM) sensor. *Heliyon* 2022; **8**, e09401.

[5] F Fauzi, A Rianjanu, I Santoso and K Triyana. Gas and humidity sensing with quartz crystal microbalance (QCM) coated with graphene-based materials - A mini-review. *Sensors Actuators A Phys.* 2021; **330**, 112837.

[6] G Xie, P Sun, X Yan, X Du and Y Jiang. Fabrication of methane gas sensor by layer-by-layer self-assembly of polyaniline/PdO ultra-thin films on quartz crystal microbalance. *Sensors Actuators B Chem.* 2010; **145**, 373-7.

[7] HM Hussien and MH Shinen. Study the sensitivity of quartz crystal microbalance (QCM) sensor coated with different thickness for determination vapors of ethanol, propanol, hexane and benzene. *Chem. Mater. Res.* 2013; **3**, 61-5.

[8] H Xu and J Zhang. Development of quartz crystal microbalance sensor modified by nano-structured polyaniline for detecting the plasticizer in gaseous state. *Sensors Transducers* 2014; **163**, 235-9.

[9] X Yu, X Chen, X Chen, X Zhao, X Yu and X Ding. Digital ammonia gas sensor based on quartz resonator tuned by interdigital electrode coated with polyaniline film. *Org. Electr*. 2020; **76**, 105413.

[10] D Zhang, Z Kang, X Liu, J Guo and Y Yang. Highly sensitive ammonia sensor based on PSS doped ZIF-8-derived porous carbon/polyaniline hybrid film coated on quartz crystal microbalance. *Sensors Actuators B Chem.* 2022; **357**, 131419.

[11] NP Putri, DW Pravitasari, FA Aziz, Maulidiah, DJDH Santjojo, Masruroh and SP Sakti. Solvent effect on viscoelastic behaviour and morphology of polyaniline coating at QCM sensor. *J. Phys. Conf. Ser*. 2019; **1417**, 012002.

[12] EIP Rahayu and NP Putri. The effect of solution concentration and deposition time on viscoelasticity and morphology of polyaniline coating. *J. Phys. Conf. Ser*. 2020; **1491**, 012050.

[13] D Zhang, D Wang, P Li, X Zhou, X Zong and G Dong. Facile fabrication of high performance QCM humidity sensor based on layer-by-layer self-assembled polyaniline/graphene oxide nanocomposite film. *Sensors Actuators B Chem.* 2018; **255**, 1869-77.

[14] NP Putri, E Yulisetiana, DJDH Santjojo, Masruroh and SP Sakti. Effect of evaporation deposition time on thickness and impedance value of polyaniline layers. *J. Phys. Conf. Ser.* 2021; **1805**, 012035.

[15] D Zhang, D Wang, X Zong, G Dong and Y Zhang. High-performance QCM humidity sensor based on graphene oxide/tin oxide/polyaniline ternary nanocomposite prepared by in-situ oxidative polymerization method. *Sensors Actuators B Chem.* 2018; **262**, 531-41.

[16] I Sa'diyah and NP Putri. The effects of potentiostat scan rate variation on impedance value, topography, and morphology of the polyaniline thin film. *J. Phys. Sci. Eng.* 2021; **6**, 46-54.

[17] HJNPD Mello and M Mulato. Influence of galvanostatic electrodeposition parameters on the structure-property relationships of polyaniline thin films and their use as potentiometric and optical pH sensors. *Thin Solid Films* 2018; **656**, 14-21.

[18] L Hou, X Zhi, W Zhang and H Zhou. Boosting the electrochemical properties of polyaniline by one-step co-doped electrodeposition for high performance flexible supercapacitor applications. *J. Electroanal. Chem*. 2020; **863**, 114064.

[19] T Xue, LS Loo, X Wang, SK Kwak and JM Lee. Electrodeposition of mesoporous bilayers of polyaniline supported Cu_2O semiconductor films from lyotropic liquid crystalline phase. *Chem. Eng. Sci*. 2012; **80**, 452-9.
[20] AD Jagadale, VS Jamadade, SN Pusawale and CD Lokhande. Effect of scan rate on the morphology of potentiodynamically deposited B-$Co(OH)_2$ and corresponding supercapacitive performance. *Electrochimica Acta* 2012; **78**, 92-7.
[21] A Baba, A Tian, F Stefani, C Xia, Z Wang, RC Advincula, D Johannsmann and W Knoll. Electropolymerization and doping/dedoping properties of polyaniline thin films as studied by electrochemical surface plasmon spectroscopy and by the quartz crystal microbalance. *J. Electrochem. Chem*. 2004; **562**, 95-103.
[22] MA Mohamoud, AR Hillman and I Evimov. Film mechanical resonance phenomenon during electrochemical deposition of polyaniline. *Electrochimica Acta* 2008; **53**, 6235-43.
[23] YA Ismail, JG Martinez and TF Otero. Fibroin/polyaniline microfibrous mat. Preparation and electrochemical characterization as reactive sensor. *Electrochimica Acta* 2014; **123**, 501-10.
[24] J Huang, K Wu, H Bai, H Huang, X Zhang, Y Liu and C Xiong. Facile synthesis of 3D porous polyaniline composite with MnO_2-decorated fiber morphology and enhanced electrochemical performance. *Polymer* 2022; **256**, 125235.
[25] K Sahu and A K Kar. Dependency of morphological and optical properties of electropolymerized PANI thin films on different substrate for supercapacitor applications. *Mater. Lett.* 2021; **302**, 130450.
[26] SP Sakti. Quartz crystal resonator parameter calculation based on impedance analyser measurement GRG non-linear solver. *J. Nat. A* 2014; **1**, 82-9.
[27] NP Putri, AA Fahmi, DK Daniel and SP Sakti. Determination of resonance parameters of the PANI thin film fabricated using spin coating method. *J. Phys. Conf. Ser.* 2021; **2110**, 012008.
[28] Masruroh and DJDH Santjojo. The impedance analysis of a viscoelastic petalous structured stearic acid functional layer deposited on a QCM. *Sensors* 2022; **22**, 7504.
[29] SP Sakti, Masruroh, Istiroyah, DD kamasi and TN Zafirah. Ultra thick polystyrene coating on quartz crystal microbalance sensor. *Mater. Today Proceed*. 2021; **44**, 3217-20.
[30] I Burda. Advanced impedance spectroscopy for QCM sensor in liquid medium. *Sensors* 2022; **22**, 2337.
[31] SP Sakti, Masruroh, DD Kamasi and NF Khusnah. Stearic acid coating material loading effect to Quartz Crystal Microbalance sensor. *Mater. Today Proc.* 2019; **13**, 53-8.
[32] E Belarb, VM Blas-Ferrando, M Haro, H Maghraoui-Meherzi and S Gimenez. Electropolymerized polyaniline: A promising hole selesctive contact in organic photoelectrochemical cells. *Chem. Eng. Sci.* 2016; **154**, 143-9.
[33] P Chulkin and M Lapkowski. An insight into ionic conductivity of polyaniline thin films. *Materials* 2020; **13**, 2877.